BULLETIN OF THE POLISH ACADEMY OF SCIENCES
TECHNICAL SCIENCES, Vol. 72(5), 2024, Article number: e150805
DOI: 10.24425/bpasts.2024.150805

Robust fault-tolerant control with dynamic event-triggered mechanism based on observer for nonlinear switched systems

Xiaohan WANG and Xingjian FU*

School of Automation, Beijing Information Science and Technology University, Beijing, China

Abstract. In this paper, a robust fault-tolerant control with a dynamic event-triggered mechanism based on the observer is proposed for a nonlinear switched system with faults, external disturbances, and uncertainties. A first-order filter is utilized to equate sensor faults to actuator faults, and the augmented system is constructed. An adaptive observer with H_∞ performance is designed based on the augmented system. The condition that the state error and fault error of the adaptive observer are uniformly bounded is given. To save communication resources and reduce the transmission of unnecessary information, an improved dynamic event-triggered mechanism is designed by introducing a fixed threshold and defining a sampling error function based on the observed state and the actual state. This mechanism can further expand the triggering time interval and effectively avoid the Zeno behavior. According to the observed state and real-time fault estimation information at the triggering moment, a fault-tolerant controller for the switched system based on the dynamic event-triggered mechanism is proposed, and the conditions for asymptotic stability of the closed-loop system are provided. Finally, the validity of the proposed method is verified by application simulation for the variant aircraft switched system.

Keywords: switched system; adaptive fault observer; robust H_∞ control; fault-tolerant control; dynamic event-triggered mechanism.

1. INTRODUCTION

With the increasing complexity of industrial systems, actuator or sensor faults are inevitable during operation. It will lead to a degradation or deterioration in the performance of the control system. This makes the need for reliability, security, and stability of the system more and more urgent. Fault-tolerant control aims to design and implement control strategies that can maintain stable system operation in the event of faults. It is of great significance to design a fault-tolerant controller that can stabilize the system when a fault occurs [1–4]. In [1], an adaptive state feedback control method is proposed for uncertain nonlinear switched systems based on the backstepping technique, and the global stability of the closed-loop system in case of actuator fault is achieved. An adaptive neural fault-tolerant control strategy is proposed in [2] utilizing a command filter approach for a class of nonlinear switched systems. By using a neural network, the unknown nonlinear function of the system under consideration is approximated while its unmeasurable states are estimated by building a switched observer. In [3], a fault-tolerant control scheme is proposed for a class of nonlinear systems with unmatched disturbance and actuator faults. The output tracking error is asymptotically converged to zero by constructing a sliding mode control law method. Currently, the study for fault-tolerant control mainly focuses on dealing with actuator faults, while most of the investigation for fault-tolerant control on sensor faults focuses on the field of linear systems. The nature of sensors makes it difficult to accurately diagnose the fault magnitude. Therefore, the research on fault-tolerant control for nonlinear switched systems is more challenging. In [4], an indirect adaptive approach is proposed to investigate the problem of fault-tolerant control in the presence of actuator faults. An adaptive controller is designed to compensate for faults and disturbances, ensuring that the system remains asymptotically stable under both normal and fault conditions.

In recent years, observer-based fault estimation has received extensive attention from scholars [5–7] The main objective in [5] is to design controllers and observers in an integrated manner. The state and fault observers are designed to estimate the state and actuator faults. The fault-tolerant controllers are developed based on the observers to stabilize the system. In [6], a sliding mode observer (SMO) is designed to generate residual signals and compare them with a given threshold to detect whether a fault occurs in the system or not. In [7], an adaptive fault observer based on the approximation technique of fuzzy logic systems is designed to estimate both faults and states simultaneously. Based on the estimated information, an observer-based fault-tolerant controller is designed.

Switched systems, as a class of hybrid systems consisting of a series of subsystems and switching rules between subsystems, have been widely used in practical engineering, such as robot power systems, DC/DC converters, aircraft control systems [8–11], and many other fields. Investigations on switched systems have focused on the stability analysis of the system. Even

*e-mail: fxj@bistu.edu.cn

Manuscript submitted 2024-12-26, revised 2024-04-22, initially accepted for publication 2024-06-08, published in September 2024.

if there is an unstable subsystem, the system stability can still be ensured by designing suitable switching control signals [12–15]. For switched systems under arbitrary or constrained switching signals, the common Lyapunov function, multiple Lyapunov functions, and the average dwell time method have been proposed to study the system stability [16–18]. With the rapid development of computer network technology, network control systems have become an extremely important research topic in the control field. Most of the switched systems rely on the network for information transmission. Therefore, for the switched system, the introduction of an event-triggered mechanism is very necessary.

The event-triggered mechanism can effectively reduce communication and computation resources and avoid redundant data transmission. Currently, the application of event-triggered mechanisms has been studied by many researchers, such as fault diagnosis [19, 20], system control [21–24], and filtering [25]. Compared to static event-triggered mechanisms, dynamic event-triggered mechanisms have also made great progress in recent years [26–29]. In [27], the problem of adaptive event-triggered fault-tolerant consistency for general linear multi-agent systems is studied. The self-regulation of the event-triggered mechanism is improved by introducing an adaptive function into the trigger function, which makes the trigger threshold function dependent on both state and time. In [28], the system stabilization with time delay based on dynamic event-triggered intermittent control is studied. A dynamic event-triggered intermittent control scheme with input delay is proposed based on the minimum activation time rate related to time delay. A dynamic event-triggered mechanism for fault-tolerant control of linear systems is proposed in [29], where the dynamic threshold consists of the instantaneous and mean errors and their boundaries.

Compared with static event-triggered mechanisms, dynamic event-triggered mechanisms often have larger trigger intervals and fewer triggering times while ensuring system performance. However, there are relatively few research results on fault-tolerant control for switched systems under dynamic event-triggered mechanisms. In [30], the robust fault-tolerant control of nonlinear switched systems with actuator faults and disturbances under static event-triggered control strategies is investigated. The effect of actuator faults is eliminated by an adaptive estimation of an unknown upper bound on the uncertain parameters. The designed controller ensures that the signals for the closed-loop switched system are uniformly bounded. However, the control method will no longer be applicable if the sensor fault occurs. Based on the above analysis, in this paper, robust fault-tolerant control of nonlinear switched systems based on dynamic event-triggered mechanisms is investigated. The main contributions are summarized as follows: (1) For the nonlinear switched system with actuator faults, sensor faults, and external disturbances, a first-order filter is used to equate sensor faults to actuator faults, and an adaptive observer with H_∞ performance is designed. The asymptotic estimation of the system fault is achieved by the adaptive fault algorithm. The conditions in which the state error and fault error for the adaptive observer are uniformly bounded are given. (2) An improved dynamic event-triggered mechanism is designed by introducing a fixed threshold and defining a sampling error function based on the observed state and the actual state. This triggering mechanism can further expand the triggering time interval and effectively avoid Zeno behavior. (3) Based on the observed state and real-time fault estimation at the triggering moment, the design of the fault-tolerant controller for the switched system based on the dynamic event-triggered mechanism is proposed, and the conditions for the asymptotic stabilization of the closed-loop system are given. Finally, the validity of the proposed method is verified by application simulation of a variant aircraft switched system.

The paper is structured as follows: the problem description is given in Section 2. The adaptive observer design is presented in Section 3. Dynamic event-triggered mechanism with robust fault-tolerant controller design for nonlinear switched systems is presented in Section 4. Simulation results are given in Section 5 to illustrate the effectiveness of the approach. Finally, conclusions are presented in Section 6.

2. PROBLEM DESCRIPTION

Consider the following nonlinear switched system:

$$\begin{aligned} \dot{x}(t) &= A_\sigma x(t) + B_\sigma u(t) + E_\sigma S_a(t) + f_\sigma(x,t) + D_\sigma \omega(t), \\ y(t) &= C_\sigma x(t) + M_\sigma S_f(t), \end{aligned} \tag{1}$$

where $\sigma\colon R^+ \to N\{1,2,\ldots,n\}$ is the switched law, which is a piecewise constant function that depends on the state or time. $y(t)$, $u(t)$, $x(t)$, $S_a(t)$, $S_f(t)$, and $\omega(t)$ represent output vector, input vector, state vector, actuator faults, sensor faults, and external disturbances in the system, respectively. A_σ, B_σ, C_σ, D_σ, E_σ, and M_σ are matrices of known real constants with appropriate dimensions.

Assumption 1. The time-varying fault function and external disturbances are bounded and satisfy:

$$\begin{aligned} \|S_f(t)\| &\le \bar{S}_f, \\ \|S_a(t)\| &\le \bar{S}_a, \\ \|\omega(t)\| &\le \bar{\omega}. \end{aligned}$$

Assumption 2. For any given $\sigma \in N$, f_σ is a known nonlinear function that satisfies the global Lipschitz condition, for all $t \ge 0$, there is

$$\|f_\sigma(x,t)\| \le \theta \|x_1 - x_2\|,$$

where θ is the known Lipschitz constant.

Assumption 3. (A_σ, B_σ) is controllable, (A_σ, C_σ) is observable.

Lemma 1. [31] For any matrices A and B with appropriate dimensions, the following inequality holds:

$$A^T B + B^T A \le \gamma A^T A + \frac{1}{\gamma} B^T B.$$

The new state variable $\xi(t)$ is chosen as a first-order low-pass filter for the output signal:

$$\dot{\xi}(t) = -A_f \xi(t) + A_f y(t), \tag{2}$$

where $\xi(t)$ is the filter state vector and A_f is the symmetric positive definite filter matrix. Bringing the output equation in equation (1) into equation (2), one can get

$$\dot{\xi}(t) = -A_f\xi(t) + A_f C_\sigma x(t) + A_f M_\sigma S_f(t). \tag{3}$$

Next, the Lipschitz nonlinear switched system (1) is combined with equation (3) to obtain the augmented system, defined as follows:

$$\begin{aligned} \dot{\tilde{x}}(t) &= \tilde{A}_\sigma\tilde{x}(t) + \tilde{B}_\sigma u(t) + \tilde{E}_\sigma S(t) + \tilde{f}_\sigma(\tilde{x},t) + \tilde{D}_\sigma\omega(t), \\ \tilde{y}(t) &= \tilde{C}_\sigma\tilde{x}(t), \end{aligned} \tag{4}$$

where

$$\tilde{x}(t) = \begin{bmatrix} x(t) \\ \xi(t) \end{bmatrix}, \qquad \tilde{A}_\sigma = \begin{bmatrix} A_\sigma & 0 \\ A_f C_\sigma & -A_f \end{bmatrix},$$
$$\tilde{B}_\sigma = \begin{bmatrix} B_\sigma \\ 0 \end{bmatrix}, \qquad \tilde{E}_\sigma = \begin{bmatrix} E_\sigma & 0 \\ 0 & A_f M_\sigma \end{bmatrix},$$
$$S(t) = \begin{bmatrix} S_a(t) \\ S_f(t) \end{bmatrix}, \qquad \tilde{f}_\sigma(\tilde{x},t) = \begin{bmatrix} f_\sigma(x,t) \\ 0 \end{bmatrix},$$
$$\tilde{D}_\sigma = \begin{bmatrix} D_\sigma \\ 0 \end{bmatrix}, \qquad \tilde{C}_\sigma = \begin{bmatrix} 0 & C_\sigma \end{bmatrix}.$$

Remark 1. Since sensors are often located in the feedback channel in the control loop, they cannot rely on feedback mechanisms to regulate disturbances like components in the forward channel. Moreover, when an observer is designed, the inputs and outputs of the system are usually needed to observe the state, and the outputs are often measured by sensors, so the true state cannot be observed if the sensors fail. Therefore, in this paper, sensor faults are dealt with here by equating sensor faults to actuator faults by utilizing a form of first-order filter.

Assumption 4. The fault signal $S(t)$ and its derivative of the augmented system are bounded

$$\begin{aligned} \|S(t)\| &\le \bar{S}, \\ \|\dot{S}(t)\| &\le \bar{S}_1. \end{aligned}$$

Lemma 2. [32] For the scalar μ and symmetric positive definite matrices $G > 0$, the following inequality holds:

$$2x^T y \le \frac{1}{\mu}x^T G x + \mu y^T G^{-1} y, \quad x, y \in R.$$

3. ADAPTIVE OBSERVER DESIGN

For the augmented system (4), the structure of the adaptive observer is defined as:

$$\begin{aligned} \dot{\hat{\tilde{x}}}(t) &= \tilde{A}_\sigma\hat{\tilde{x}}(t) + \tilde{B}_\sigma u(t) + \tilde{E}_\sigma\hat{S}(t) + \tilde{f}_\sigma(\hat{\tilde{x}},t) \\ &\quad + L\left(\tilde{y}(t) - \hat{\tilde{y}}(t)\right), \\ \tilde{y}(t) &= \tilde{C}_\sigma\hat{\tilde{x}}(t), \end{aligned} \tag{5}$$

where $\hat{\tilde{x}}(t)$ and $\hat{\tilde{y}}(t)$ represent the state and output vectors of the observation, $\hat{S}(t)$ denotes the observed fault, $\tilde{f}_\sigma(\hat{\tilde{x}},t)$ denotes the Lipschitz nonlinear function associated with the observed state $\hat{\tilde{x}}(t)$, and L is the observer gain matrix to be designed.

Define the state error function, the fault error function, and the output error function, respectively.

$$\begin{aligned} e_x(t) &= \tilde{x}(t) - \hat{\tilde{x}}(t), \\ e_f(t) &= S(t) - \hat{S}(t), \\ e_y(t) &= \tilde{y}(t) - \hat{\tilde{y}}(t). \end{aligned}$$

Taking the derivative of the error function $e_x(t)$ with respect to time and substituting equation (1) and equation (5) yields:

$$\begin{aligned} \dot{e}_x(t) &= \left(\tilde{A}_\sigma - L\tilde{C}_\sigma\right)e(t) + \tilde{E}_\sigma e_f(t) \\ &\quad + \tilde{f}_\sigma(\tilde{x},t) - \tilde{f}_\sigma(\hat{\tilde{x}},t) + \tilde{D}_\sigma\omega(t). \end{aligned} \tag{6}$$

Theorem 1. Under Assumption 1 to Assumption 4, for a given constant $\gamma_0 > 0$, if the adaptive observer (5) is introduced into the system (4), and there exists a symmetric positive definite matrix $P_1 = P_1^T > 0$, scalar $\mu_1 > 0$, and symmetric matrix H_1, the following conditions hold:

$$\Psi = \begin{bmatrix} \psi_1 & 0 & \theta P_1 & PD_\sigma \\ * & \mu_1 H_1 & 0 & 0 \\ * & * & -I & 0 \\ * & * & * & -\gamma_0^2 I \end{bmatrix} < 0, \tag{7}$$

$$R_1 C_\sigma = E_\sigma^T P_1, \tag{8}$$

where

$$\begin{aligned} \psi_1 &= \left(\tilde{A}_\sigma - L\tilde{C}_\sigma\right)^T P_1 + P_1\left(\tilde{A}_\sigma - L\tilde{C}_\sigma\right) + \tilde{C}_\sigma^T\tilde{C}_\sigma + I, \\ \delta &= \bar{S}_1^2\lambda_{\max}(\kappa^{-1}H^{-1}\kappa^{-1}). \end{aligned}$$

Adaptive fault estimation algorithm:

$$\dot{\hat{S}}(t) = \kappa R_1 e_y(t), \tag{9}$$

where κ is the adaptive law. Then, the adaptive observer (5) can ensure that $e_x(t)$ and $e_f(t)$ are uniformly bounded, and the H_∞ performance index is no greater than γ_0.

Proof. . Choose a Lyapunov function:

$$V_i(t) = e_x^T(t)P_1 e_x(t) + e_f^T(t)\kappa^{-1}e_f(t). \tag{10}$$

If the i-th subsystem is in the activated state, one can get

$$\begin{aligned} &\dot{V}_i(t) + e_y^T(t)e_y(t) - \gamma_0^2\omega^T(t)\omega(t) \\ &\le e_x^T(t)\left[\left(\tilde{A}_i - L\tilde{C}_i\right)^T P_1 + P_1\left(\tilde{A}_i - L\tilde{C}_i\right)\right]e_x(t) \\ &\quad + 2e_x^T(t)P_1\tilde{E}_i e_f(t) + 2e_x^T(t)P_1\left[\tilde{f}_i(\tilde{x},t) - \tilde{f}_i(\hat{\tilde{x}},t)\right] \\ &\quad + 2e_x^T(t)P_1\tilde{D}_i\omega(t) + 2e_f^T(t)\kappa^{-1}\dot{e}_f(t) \\ &\quad + e_y^T(t)e_y(t) - \gamma_0^2\omega^T(t)\omega(t). \end{aligned} \tag{11}$$

According to equation (8), one can get

$$\begin{aligned}
&\dot{V}_i(t)+e_y^T(t)e_y(t)-\gamma_0^2\omega^T(t)\omega(t)\\
&\quad\le e_x^T(t)\left[\left(\tilde{A}_i-L\tilde{C}_i\right)^T P_1+P_1\left(\tilde{A}_i-L\tilde{C}_i\right)\right]e_x(t)\\
&\qquad+2e_x^T(t)P_1\tilde{E}_i e_f(t)+2e_x^T(t)P_1\left[\tilde{f}_i(\tilde{x},t)-\tilde{f}_i(\hat{\tilde{x}},t)\right]\\
&\qquad+2e_x^T(t)P_1\tilde{D}_i\omega(t)+2e_f^T(t)\kappa^{-1}\dot{S}(t)-2e_f^T(t)R_1e_y(t)\\
&\qquad+e_y^T(t)e_y(t)-\gamma_0^2\omega^T(t)\omega(t), \qquad (12)\\
&2e_x^T(t)P_1\tilde{E}_i e_f(t)=2e_f^T(t)R_1\tilde{C}_i e_x(t). \qquad (13)
\end{aligned}$$

By Assumption 2

$$\begin{aligned}
&2e_x^T(t)P_1\left[\tilde{f}_i(\tilde{x},t)-\tilde{f}_i(\hat{\tilde{x}},t)\right]\\
&\qquad\le\theta^2e_x^T(t)P_1^TP_1e_x(t)+e_x^T(t)e_x(t).. \qquad (14)
\end{aligned}$$

From Lemma 1

$$\begin{aligned}
2e_x^TP_1\tilde{D}_i\omega(t)\le&\frac{1}{\gamma_0^2}e_x^T(t)P_1\tilde{D}_i\tilde{D}_i^TP_1e_x(t)\\
&+\gamma_0^2\omega^T(t)\omega(t). \qquad (15)
\end{aligned}$$

From the Assumption 4 and the Lemma 2, one can obtain

$$\begin{aligned}
2e_f^T(t)\kappa^{-1}\dot{S}(t)&\le\mu_1e_f^T(t)H_1e_f(t)+\frac{\bar{S}_1^2}{\mu_1}\kappa^{-1}H_1^{-1}\kappa^{-1}\\
&\le\mu_1e_f^T(t)H_1e_f(t)+\frac{\bar{S}_1^2}{\mu_1}\lambda_{\max}(\kappa^{-1}H_1^{-1}\kappa^{-1}). \qquad (16)
\end{aligned}$$

Bringing the equations (13)–(16) into equation (12) yields

$$\begin{aligned}
&\dot{V}_i(t)+e_y^T(t)e_y(t)-\gamma_0^2\omega^T(t)\omega(t)\\
&\quad\le e_x^T(t)\left[\left(\tilde{A}_i-L\tilde{C}_i\right)^T P_1+P_1\left(\tilde{A}_i-L\tilde{C}_i\right)\right]e_x(t)\\
&\qquad+\theta^2e_x^T(t)P_1^TP_1e_x(t)+e_x^T(t)e_x(t)\\
&\qquad+\frac{1}{\gamma_0^2}e_x^T(t)P_1\tilde{D}_i\tilde{D}_i^TP_1e_x(t)+\gamma_0^2\omega^T(t)\omega(t)\\
&\qquad+\mu_1e_f^T(t)H_1e_f(t)+\frac{\bar{S}_1^2}{\mu_1}\lambda_{\max}(\kappa^{-1}H_1^{-1}\kappa^{-1})\\
&\qquad+e_x^T(t)\tilde{C}_i^T\tilde{C}_ie_x(t)-\gamma_0^2\omega^T(t)\omega(t). \qquad (17)
\end{aligned}$$

□

The matrix M is defined as follows:

$$\begin{aligned}
\mathrm{M}=&e_x^T(t)\left[\left(\tilde{A}_i-L\tilde{C}_i\right)^T P_1+P_1\left(\tilde{A}_i-L\tilde{C}_i\right)\right]e_x(t)\\
&+\theta^2e_x^T(t)P_1^TP_1e_x(t)+e_x^T(t)e_x(t)+\mu_1e_f^T(t)H_1e_f(t)\\
&+e_x^T(t)\tilde{C}_i^T\tilde{C}_ie_x(t)+\frac{1}{\gamma_0^2}e_x^T(t)P_1\tilde{D}_i\tilde{D}_i^TP_1e_x(t)+\frac{1}{\mu_1}\delta\\
=&\begin{bmatrix}e_x(t)\\e_f(t)\end{bmatrix}^T\begin{bmatrix}\Psi_1&0\\0&\mu_1H_1\end{bmatrix}\begin{bmatrix}e_x(t)\\e_f(t)\end{bmatrix}+\frac{1}{\mu_1}\delta, \qquad (18)
\end{aligned}$$

where

$$\begin{aligned}
\varepsilon(t)=&\begin{bmatrix}e_x(t)\\e_f(t)\end{bmatrix},\quad H=\begin{bmatrix}\Psi_1&0\\0&\mu_1H_1\end{bmatrix},\\
\Psi_1=&\left(\tilde{A}_i-L\tilde{C}_i\right)^TP_1+P_1\left(\tilde{A}_i-L\tilde{C}_i\right)\\
&+\theta^2P_1^TP_1+\frac{1}{\gamma_0^2}P_1\tilde{D}_i\tilde{D}_i^TP_1+\tilde{C}_i\tilde{C}_i^T+I.
\end{aligned}$$

Equation (18) can be written as

$$Q=\varepsilon^T(t)H\varepsilon(t)+\frac{1}{\mu_1}\delta. \qquad (19)$$

Based on the Schur complement, the matrix H is equivalent to

$$\Psi=\begin{bmatrix}\psi_1&0&\theta P_1&PD_\sigma\\*&\mu_1H_1&0&0\\*&*&-I&0\\*&*&*&-\gamma_0^2I\end{bmatrix}, \qquad (20)$$

when $H<0$, then $\delta<-\mu_1^2\lambda_{\max}(-H)\|\varepsilon\|^2$. Based on Lyapunov stability theory, it follows that $\dot{V}_i(t)+e_y^T(t)e_y(t)-\gamma_0^2\omega^T(t)\omega(t)<0$, and for the initial condition $V_i(0)=0, V_i(\infty)>0$, by sorting and integrating, we can obtain equation (21)

$$\int_0^t e_y^T(t)e_y(t)\,\mathrm{d}t<\gamma_0^2\int_0^t\omega^T(t)\omega(t)\,\mathrm{d}t. \qquad (21)$$

Then the state and fault estimation errors $(e_x(t), e_f(t))$ are uniformly bounded, and the H_∞ performance index is not greater than γ_0.

Remark 2. According to the fault estimation algorithm (9), the change rate of fault estimation depends on the output error and adaptive law κ. For different application scenarios, adjusting the adaptive law κ can reasonably estimate different faults.

4. DYNAMIC EVENT-TRIGGERED ROBUST FAULT-TOLERANT CONTROLLER DESIGN

In this section, dynamic event-triggered conditions are given and inspired by [26], an internal dynamic variable is designed based on the static event-triggered mechanism to obtain a longer triggering time interval compared to the static event-triggered mechanism. The specific scheme adopted is as follows:

$$\begin{aligned}
&t_0=0,\\
&\tilde{t}_{k+1}=\inf\left\{t>t_k|\ \phi(t)+r_0+\partial\left(\varepsilon_1\|\widehat{x}(t)\|-\|\widehat{e}(t)\|\right)\le0\right\},
\end{aligned} \qquad (22)$$

where $\partial>0$, $r_0>0$.

The dynamic variable $\phi(t)$ is defined as:

$$\dot{\phi}(t)=-\chi\phi(t)+\varepsilon_1\|\widehat{x}(t)\|-\|\widehat{e}(t)\|. \qquad (23)$$

Initial conditions $\phi(0)\ge\phi_0$, $0<\chi<1$.

Define the event-triggered error based on the observed state:

$$\widehat{e}(t) = \tilde{x}(\tilde{t}_k) - \hat{\tilde{x}}(\tilde{t}_k), \tag{24}$$

where $\tilde{t}_k$ is the event-triggered transient.

Remark 3. χ describes the attenuation rate of filtering. The smaller χ is, the more filtered signals will be. Therefore, χ should be as small as possible. ε_1 reflects the tightness of the event triggering. A larger ε_1 will result in greater tolerance for error $\widehat{e}(t)$, which will result in a smaller number of triggers.

Consider applying (22) to the robust fault-tolerant controller that will be designed. Assuming that n samples occur on the interval $[t_i, t_{i+1})$, then

$$u(t) = \begin{cases} u(\tilde{t}_k), & t \in [t_i,\ \tilde{t}_{k+1}), \\ u(\tilde{t}_{k+1}), & t \in [\tilde{t}_{k+1},\ \tilde{t}_{k+2}), \\ \cdots & \\ u(\tilde{t}_{k+n}), & t \in [\tilde{t}_{k+n},\ t_{i+1}). \end{cases} \tag{25}$$

Next, the fault-tolerant controller is designed by utilizing the observed state and real-time fault estimation information obtained in Section 3.

Assumption 5. $\operatorname{rank}(B, E) = \operatorname{rank}(B)$, i.e., there exists a matrix such that

$$\left(I - BB^{+}\right)E = 0.$$

The following fault-tolerant controllers based on observation information are considered:

$$u(t) = -K\hat{\tilde{x}}(t) - \tilde{B}_{\sigma}^{+}\tilde{E}_{\sigma}\hat{S}(t), \tag{26}$$

where K is the control gain and $\tilde{B}_{\sigma}^{+}$ is the generalized right inverse of matrix $\tilde{B}_{\sigma}$.

Bringing equation (26) into the augmented system (3) yields

$$\begin{aligned} \dot{\tilde{x}}(t) &= \tilde{A}_{\sigma}\tilde{x}(t) - \tilde{B}_{\sigma}K\hat{\tilde{x}}(t) - \tilde{E}_{\sigma}\hat{S}(t) + \tilde{E}_{\sigma}S(t) \\ &\quad + \tilde{f}_{\sigma}(\tilde{x},t) + \tilde{D}_{\sigma}\omega(t) \\ &= \tilde{A}_{\sigma}\tilde{x}(t) - \tilde{B}_{\sigma}K\hat{\tilde{x}}(t) + \tilde{B}_{\sigma}K\tilde{x}(t) - \tilde{B}_{\sigma}K\tilde{x}(t) \\ &\quad + \tilde{f}_{\sigma}(\tilde{x},t) + \tilde{D}_{\sigma}\omega(t) + \tilde{E}_{\sigma}e_f(t) \\ &= \left(\tilde{A}_{\sigma} - \tilde{B}_{\sigma}K\right)\tilde{x}(t) + \tilde{B}_{\sigma}Ke_x(t) + \tilde{E}_{\sigma}e_f(t) \\ &\quad + \tilde{f}_{\sigma}(\tilde{x},t) + \tilde{D}_{\sigma}\omega(t). \end{aligned} \tag{27}$$

Let

$$d(t) = \begin{bmatrix} e_x^T(t) & \omega^T(t) & e_f^T(t) \end{bmatrix}^T,$$
$$\tilde{M} = \begin{bmatrix} \tilde{B}_{\sigma}K & \tilde{D}_{\sigma} & \tilde{E}_{\sigma} \end{bmatrix}.$$

Then equation (27) can be rewritten as

$$\dot{\tilde{x}}(t) = \left(\tilde{A}_{\sigma} - \tilde{B}_{\sigma}K\right)\tilde{x}(t) + \tilde{M}d(t) + \tilde{f}_{\sigma}(\tilde{x},t). \tag{28}$$

Theorem 2. For the closed-loop system (28), if there exists a symmetric positive definite matrix $P_2 = P_2^T > 0$, scalars $\mu_2 > 0$, $\gamma > 0$ and a control gain matrix K such that

$$\begin{bmatrix} \Psi_2 & P_2\tilde{B}_{\sigma}K & P_2\tilde{D}_{\sigma} & P_2\tilde{E}_{\sigma} & \theta P_2 \\ * & -\gamma^2 I_n & 0 & 0 & 0 \\ * & * & -\gamma^2 I_b & 0 & 0 \\ * & * & * & -\gamma^2 I_e & 0 \\ * & * & * & * & -\mu_2 I_c \end{bmatrix} < 0. \tag{29}$$

Then the closed-loop system is asymptotically stable and has an H_∞ performance index γ that is

$$\int_0^t y^T(t)y(t)\,\mathrm{d}t < \gamma^2 \int_0^t d^T(t)d(t)\,\mathrm{d}t, \tag{30}$$

where

$$\Psi_2 = P_2\left(\tilde{A}_{\sigma} - \tilde{B}_{\sigma}K\right) + \left(\tilde{A}_{\sigma} - \tilde{B}_{\sigma}K\right)^T P_2 + \tilde{C}_{\sigma}^T\tilde{C}_{\sigma} + \mu_2\,.$$

Proof. Choose a Lyapunov function:

$$V_i(t) = \tilde{x}^T(t)P_2\tilde{x}(t), \tag{31}$$

where $P_2 = P_2^T \geq 0$. If the i_{th} subsystem is in the activated state, one can get

$$\begin{aligned} &\dot{V}_i(t) + \tilde{y}^T(t)\tilde{y}(t) - \gamma^2 d^T(t)d(t) \\ &\quad = \tilde{x}^T(t)\left[\left(\tilde{A}_i - \tilde{B}_iK\right)^T P_2 + P_2\left(\tilde{A}_i - \tilde{B}_iK\right)\right]\tilde{x}(t) \\ &\qquad + 2\tilde{x}^T(t)P_2\tilde{f}_i(\tilde{x},t) + 2\tilde{x}^T(t)P_2\tilde{M}d(t) \\ &\qquad + \tilde{y}^T(t)\tilde{y}(t) - \gamma^2 d^T(t)d(t). \end{aligned} \tag{32}$$

By Assumption 2 and Lemma 2, one has

$$2\tilde{x}^T(t)P_2\tilde{f}_i(\tilde{x},t) \leq \frac{\theta^2}{\mu_2}\tilde{x}^T(t)P_2^TP_2\tilde{x}(t) + \mu_2\tilde{x}^T(t)\tilde{x}(t). \tag{33}$$

Substituting equation (5) and equation (33) into equation (32), one obtains

$$\begin{aligned} &\dot{V}_i(t) + \tilde{y}^T(t)\tilde{y}(t) - \gamma^2 d^T(t)d(t) \\ &\quad \leq \tilde{x}^T(t)\left[\left(\tilde{A}_i - \tilde{B}_iK\right)^T P_2 + P_2\left(\tilde{A}_i - \tilde{B}_iK\right)\right. \\ &\qquad \left. + \frac{\theta^2}{\mu_2}P_2^TP_2 + \mu_2\right]\tilde{x}(t) + \tilde{x}^T(t)\tilde{C}_i^T\tilde{C}_i\tilde{x}(t) \\ &\qquad + 2\tilde{x}^T(t)P_2\tilde{M}d(t) - \gamma^2 d^T(t)d(t) \\ &\quad \leq \tilde{x}^T(t)\left[\left(\tilde{A}_i - \tilde{B}_iK\right)^T P_2 + P_2\left(\tilde{A}_i - \tilde{B}_iK\right)\right. \\ &\qquad \left. + \tilde{C}_i^T\tilde{C}_i + \frac{\theta^2}{\mu_2}P_2^TP_2 + \mu_2\right]\tilde{x}(t) \\ &\qquad + 2\tilde{x}^T(t)P_2\tilde{M}d(t) - \gamma^2 d^T(t)d(t) \\ &\quad = \begin{bmatrix} x(t) \\ d(t) \end{bmatrix}^T \begin{bmatrix} \psi_{11} & P_2\tilde{M} \\ * & -\gamma^2 I_s \end{bmatrix} \begin{bmatrix} x(t) \\ d(t) \end{bmatrix}, \end{aligned} \tag{34}$$

where

$$
\begin{aligned}
s &= n+b+e,\\
\psi_{11} &= \left(\tilde{A}_i-\tilde{B}_iK\right)^T P_2+P_2\left(\tilde{A}_i-\tilde{B}_iK\right)\\
&\quad + C_i^TC_i+\frac{\theta^2}{\mu_2}P_2^TP_2+\mu_2,\\
\Phi &= \begin{bmatrix}\psi_{11} & P_2\tilde{M}\\ * & -\gamma^2 I_s\end{bmatrix}, \qquad (35)\\
P_2\tilde{M} &= \begin{bmatrix}P_2\tilde{B}_iK & P\tilde{D}_i & P\tilde{E}_i\end{bmatrix}. \qquad (36)
\end{aligned}
$$

Utilizing equation (36), $\Phi<0$ can be rewritten as

$$
\begin{bmatrix}\psi_{11} & P_2\tilde{B}_iK & P_2\tilde{D}_i & P_2\tilde{E}_i\\ * & -\gamma^2 I_n & 0 & 0\\ * & * & -\gamma^2 I_b & 0\\ * & * & * & -\gamma^2 I_e\end{bmatrix}<0. \qquad (37)
$$

Based on Schur complement, the above inequality is equivalent to:

$$
\begin{bmatrix}\Psi_2 & P_2\tilde{B}_iK & P_2\tilde{D}_i & P_2\tilde{E}_i & \theta P_2\\ * & -\gamma^2 I_n & 0 & 0 & 0\\ * & * & -\gamma^2 I_b & 0 & 0\\ * & * & * & -\gamma^2 I_e & 0\\ * & * & * & * & -\mu_2 I_c\end{bmatrix}<0, \qquad (38)
$$

where

$$
\Psi_2 = P_2\left(\tilde{A}_i-\tilde{B}_iK\right)+\left(\tilde{A}_i-\tilde{B}_iK\right)^T P_2+\mu_2+\tilde{C}_i^T\tilde{C}_i.
$$

Equation (38) holds, i.e., $\dot{V}_i(t)+\tilde{y}^T(t)\tilde{y}(t)-\gamma^2 d^T(t)d(t)\le 0$. Similar to Theorem 1, the fact that this inequality holds implies that the closed-loop system (28) is asymptotically stable and has an H_∞ performance index γ. Therefore, equations (29) and (30) hold. □

Theorem 3. For any $\Lambda_x\ge 0$, $\Lambda_\phi\ge 0$, $\bar{\omega}\ge 0$, all positive real numbers k, there exists a strict positive lower bound on the minimum triggering interval $\alpha_{\min}$, i.e., $\tilde{t}_{k+1}-\tilde{t}_k\ge\alpha_{\min}$, for each solution in (4), $\|\tilde{x}(0)\|\le\Lambda_x$, $\|\omega\|\le\bar{\omega}$, then the lower bound of the minimum interval is given by the following equation:

$$
\alpha_{\min}\ge\frac{\varphi}{\tau}, \qquad (39)
$$

where

$$
\begin{aligned}
&\varphi=\varepsilon\Lambda_x, \qquad \varphi_1=\max\|\tilde{A}_i-L\tilde{C}_i\|,\\
&\varphi_2=\max\|\tilde{E}_i\|, \quad \varphi_3=\max\|\tilde{D}_i\|,\\
&\tau=\|\dot{\widehat{e}}(t)\|\le\varphi_1\|e_x(t)\|+\varphi_2\|e_f(t)\|+\theta\|e_x(t)\|+\varphi_3\|\bar{\omega}\|.
\end{aligned}
$$

Proof. According to Assumption 1 and Assumption 2, at the triggering interval $[\tilde{t}_k,\tilde{t}_{k+1})$, there is:

$$
\begin{aligned}
\|\dot{\widehat{e}}(t)\| &= \|\dot{e}_x(t)\|\\
&= \left\|\left(\tilde{A}_i-L\tilde{C}_i\right)e_x(t)+\tilde{E}_ie_f(t)+\tilde{f}_i(\tilde{x},t)-\tilde{f}_i(\hat{\tilde{x}},t)+\tilde{D}_i\omega(t)\right\|\\
&\le\varphi_1\|e_x(t)\|+\varphi_2\|e_f(t)\|+\theta e_x(t)+\varphi_3\|\bar{\omega}\|. \qquad (40)
\end{aligned}
$$

According to Theorem 1, $e_x(t)$ and $e_f(t)$ are uniformly bounded and have H_∞ performance index γ_0, thus

$$
\begin{aligned}
\|\dot{\widehat{e}}(t)\| &\le\varphi_1\|e_x(t)\|+\varphi_2\|e_f(t)\|\\
&\quad+\theta\|e_x(t)\|+\varphi_3\|\bar{\omega}\|=\tau. \qquad (41)
\end{aligned}
$$

Integrating the inequality (41) with the initial condition $\widehat{e}(\tilde{t}_k)=0$ yields

$$
\|\widehat{e}(t)\|\le\tau(t-\tilde{t}_k). \qquad (42)
$$

On the trigger interval $[\tilde{t}_k,\tilde{t}_{k+1})$, according to the dynamic event-triggered scheme (23), the next event will be triggered under the following conditions:

$$
r_0+\partial(\varepsilon\|\widehat{x}(t)\|-\|\widehat{e}(t)\|)=-\phi(t). \qquad (43)
$$

From Theorem 2, it is easy to obtain that:

$$
\|\widehat{x}(t)\|\le\|x(0)\|, \qquad (44)
$$

i.e.

$$
\|\widehat{x}(t)\|\le\Lambda_x. \qquad (45)
$$

Since $\phi(t)\ge 0$, $r_0\ge 0$, the event will not occur before $\|\widehat{e}(t)\|=\varepsilon\|\widehat{x}(t)\|$, and the time interval is greater than or equal to the following equation:

$$
\alpha^*_{\min}=\frac{\varphi}{\tau}. \qquad (46)
$$

The above equation is completely non-negative, the proof is complete. □

5. APPLICATION SIMULATION STUDY

To verify the effectiveness of the proposed method, in this section, a variant craft model in [33] is used for application simulation. The variant craft model used in this section is to change the flight state by switching the wingspan curvature. The specific model is represented as follows:

$$
\begin{aligned}
\dot{x}(t) &= A_\sigma x(t)+B_\sigma u(t)+E_\sigma S_a(t)+f_\sigma(x,t)+D_\sigma\omega(t),\\
y(t) &= C_\sigma\tilde{x}(t)+M_\sigma S_f(t),
\end{aligned}
$$

$x(t)=[x_1(t),x_2(t),x_3(t),x_4(t)]^T=[\Delta V_0,\Delta\beta_0,\Delta\theta_0,\Delta q_0]$ is the engine status, where V_0, β_0, θ_0, q_0 represent velocity (m/s), angle of attack (rad), pitch angle (rad), and pitch angle velocity (rad/s), respectively.

Considering a flying wing curvature f with values of 0 and 1, i.e., the initial base airfoil state, as well as the system state at

wingspan curvature $f = 1\%$, comprise a variant craft system with two subsystems. The parameters are selected as follows:

$$A_1 = \begin{bmatrix} -18 & -0.7 & 0 & 1 \\ 1.5 & -0.8 & 0 & 0 \\ 2 & -1 & -1 & 0 \\ 15 & 0 & 1 & -2.5 \end{bmatrix}, \quad B_1 = \begin{bmatrix} 9 & 0.2 \\ 1 & -1.2 \\ -1 & 1 \\ 0 & 1 \end{bmatrix},$$

$$E_1 = \begin{bmatrix} -7 \\ -2.2 \\ 0 \\ -4 \end{bmatrix}, \quad A_2 = \begin{bmatrix} -20 & -1 & 0 & 1 \\ 2 & -1 & 0 & 0 \\ 2 & -1 & -1 & 0 \\ 0 & 0 & 0 & -2 \end{bmatrix},$$

$$B_2 = \begin{bmatrix} 0.5 & 0.2 \\ 1 & -1.2 \\ -1 & 1 \\ 0 & 1 \end{bmatrix}, \quad E_2 = \begin{bmatrix} -4.1 \\ -2.2 \\ 0 \\ 1 \end{bmatrix},$$

$$D_1 = \begin{bmatrix} -2 & 2 \\ 1 & 1 \\ 0.7 & 0 \\ 0 & 0 \end{bmatrix}, \quad D_2 = \begin{bmatrix} 0.7 & 0.8 \\ 1 & 0.9 \\ 0.5 & 0 \\ 0 & 0 \end{bmatrix},$$

$$C_1 = C_2 = \begin{bmatrix} 1 & 0 & 0 & 0 \\ 0 & 1 & 0 & 0 \\ 0 & 0 & 0 & 1 \end{bmatrix},$$

$$M_1 = M_2 = \begin{bmatrix} 1 & 1 & 1 \end{bmatrix}^T.$$

Based on Theorem 1 and Theorem 2, the observer gain matrix and controller gain matrix can be obtained as follows:

$$L_1 = \begin{bmatrix} 0.4690 & -3.4532 & -0.1347 \\ 0.6863 & 2.6364 & 0.0719 \\ 0.2755 & -1.5863 & 0.0271 \\ -0.1244 & -0.5058 & 1.1170 \\ 3.5466 & 0.1900 & 0.0236 \\ -0.0879 & 3.3816 & 0.1934 \\ -0.0170 & -0.1822 & 3.5317 \end{bmatrix},$$

$$L_2 = \begin{bmatrix} 0.2396 & -4.5688 & -0.1620 \\ 1.2125 & 3.4029 & 0.1026 \\ 0.5299 & -1.1132 & 0.0366 \\ -0.3251 & -0.7317 & 1.2231 \\ 3.8260 & 0.5240 & -0.1403 \\ -0.3798 & 3.7206 & 0.0449 \\ 0.1491 & -0.0349 & 3.8026 \end{bmatrix},$$

$$K_1 = \begin{bmatrix} 1.0084 & 1.5651 & 0.8161 & 1.1737 & 0.2990 & 0.3466 & 0.2026 \\ 1.5611 & -4.2713 & 1.1753 & -0.2063 & 0.0215 & -2.1193 & 0.1491 \end{bmatrix},$$

$$K_2 = \begin{bmatrix} 10.1149 & 10.0768 & 0.8161 & 3.7878 & 1.3444 & 0.3466 & 2.5418 \\ 7.5657 & 1.9502 & 3.5891 & 2.6715 & 0.0215 & 0.8705 & -0.1990 \end{bmatrix}.$$

In this paper, the actuator fault and sensor fault are considered at the same time, and the actuator mutation fault and sensor gradual fault are considered respectively.

Case 1

1. Actuator mutation fault:

$$S_a(t) = \begin{cases} 0.01, & 0\text{ s} \le t < 3\text{ s}, \\ 0.08(1 - e^{-2(t-3)}), & 3\text{ s} \le t < 10\text{ s}. \end{cases}$$

2. Sensor gradual fault:

$$S_f(t) = b_0 \sin(2\pi f t),$$

where $b_0 = 0.05$, $f = 0.5$.

In addition, let $f_1(x,t) = 0.01 \sin x_1$, $f_2(x,t) = 0.01 \cos x_2$, $\omega = [0.02, 0.01]^T$.

The simulation parameters $\partial = 1$, $\chi = 0.8$, $\varepsilon_1 = 0.4$, $r_0 = 0.1$ are selected.

Under the initial conditions $x_1(0) = \begin{bmatrix} -2 & 1 & 0 & -1 \end{bmatrix}^T$, $x_2(0) = \begin{bmatrix} 2 & 1 & 1 & 1 \end{bmatrix}^T$, $\phi_0 = 0$, the simulation results are shown in Figs. 1–4.

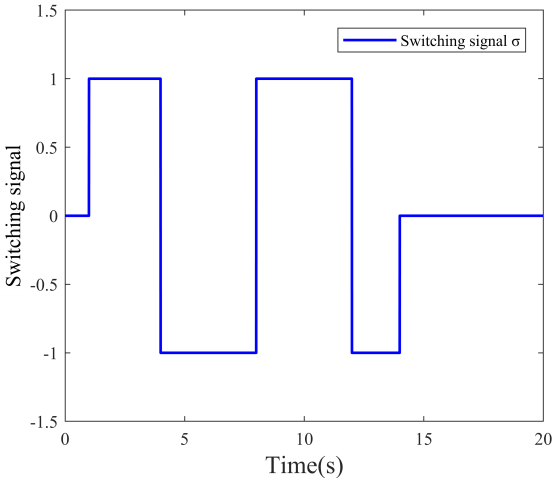

Fig. 1. Curve of switched signal $\sigma(t)$

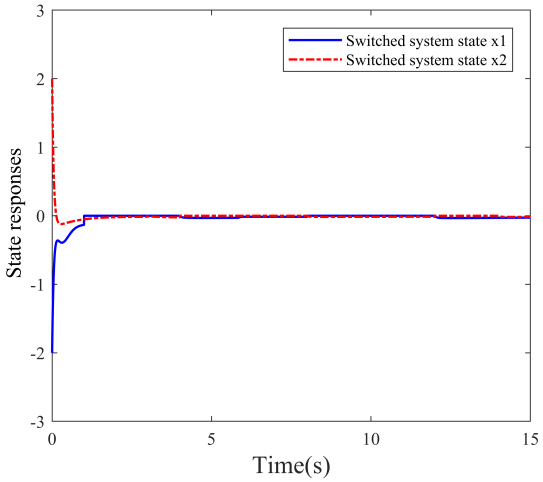

Fig. 2. State curves of the nonlinear switched system

The switched signal curve $\sigma(t)$ is shown in Fig. 1. The state response curves of the nonlinear switched system, under the action of the robust fault-tolerant controller based on the dynamic event-triggered mechanism are shown in Fig. 2.

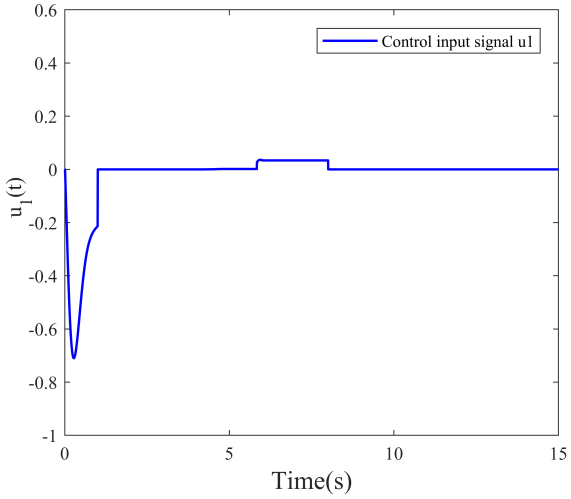

Fig. 3. Control input curve for subsystem 1

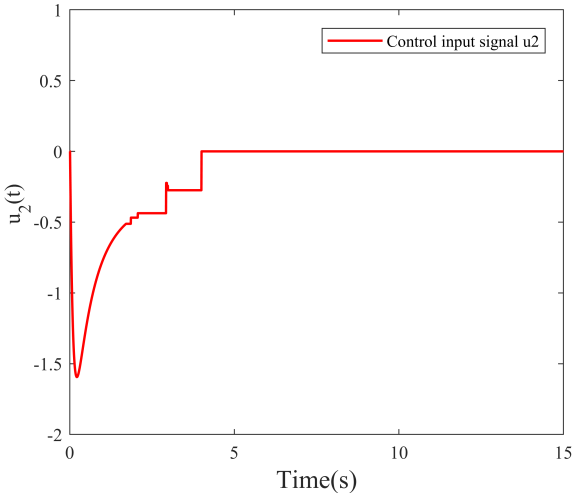

Fig. 4. Control input curve for subsystem 2

The effects of actuator and sensor faults are effectively compensated by the designed control method. Furthermore, the system is ensured to sustain its desired performance despite the presence of external disturbances. It can be seen that the state response curves $x_i(t)$ of the two subsystems with different initial conditions can rapidly converge to zero within 5 s. Additionally, it can be ensured that the system maintains an ideal steady state even after prolonged operation.

Case 2

1. Actuator mutation fault:

$$S_a(t) = \begin{cases} 0.1, & 0\text{ s} \le t < 3\text{ s}, \\ 0.4(1-e^{-2(t-3)}), & 3\text{ s} \le t < 10\text{ s}. \end{cases}$$

2. Sensor gradual fault:

$$S_f(t) = b_0 \sin(2\pi f t),$$

where $b0 = 0.5$, $f = 0.5$.

Let $f_1(x,t) = 0.2\sin x_1$, $f_2(x,t) = 0.2\cos x_2$, $\omega = [0.2, 0.3]^T$.

This time, the corresponding state curves of the system are shown in Fig. 5. The control input curves for subsystems 1 and 2 are shown in Fig. 6 and Fig. 7.

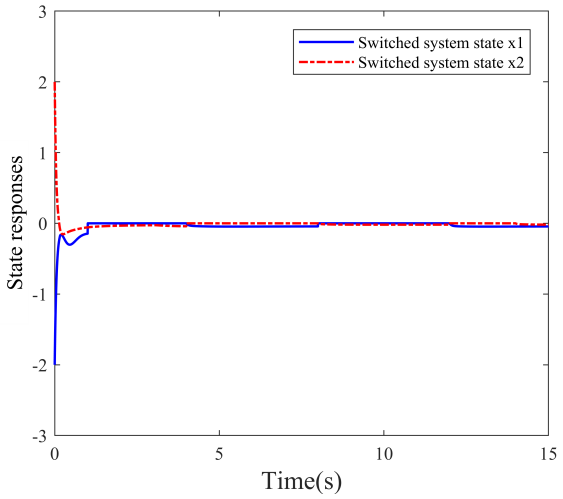

Fig. 5. State curves of the nonlinear switched system

As shown in Fig. 5, by enhancing the magnitude of the disturbances and the amplitude of the faults, it can be seen that the systems still have the desired performance, and the state response curves can also quickly converge to 0 within 5 s and continue to run stably. Therefore, the robust fault-tolerant control algorithm designed in this paper can achieve stability and maintain robustness in the variant aircraft system.

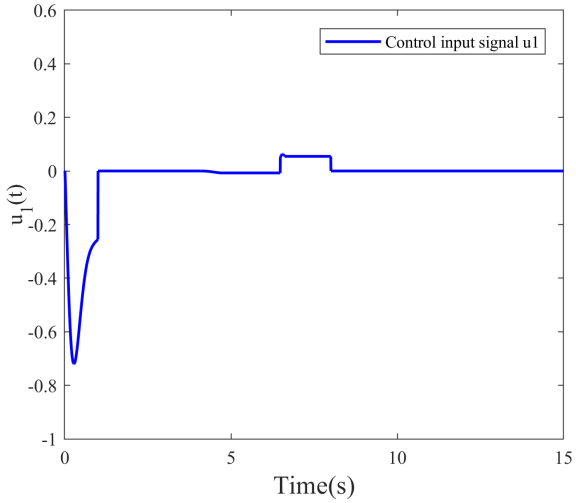

Fig. 6. Control input curve for subsystem 1

The observed state curves of the nonlinear switched system are shown in Fig. 8. The dynamic event-triggered scheme designed based on the relationship between this observed state and

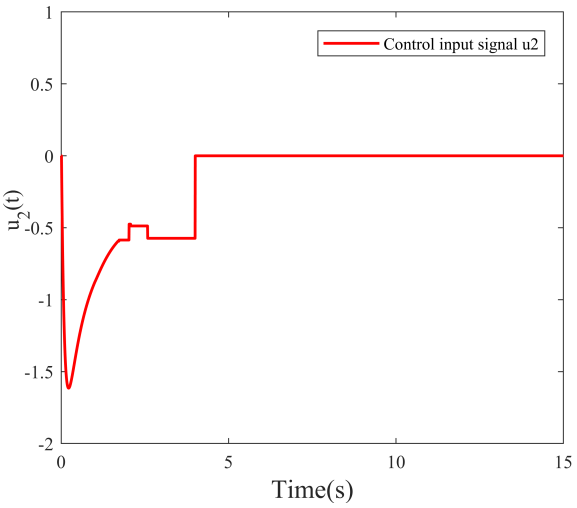

Fig. 7. Control input curve for subsystem 2

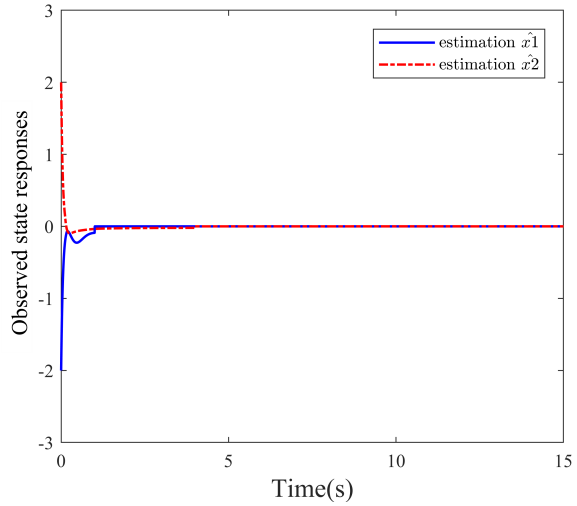

Fig. 8. Observed state curves of the nonlinear switched system

the state of the actual system can effectively reduce the number of aircraft data transmissions and communication. The system runs for 15 s and transmits data a total of 2000 times when the event-triggered mechanism is not used. Under the static event-triggered mechanism, the two subsystems transmit data 371 and 359 times, respectively. The total number of transmissions is reduced by 81.4%, and system performance can also be maintained, as shown in Fig. 9b. In Fig. 9a, the two subsystems transmit data 193 and 199 times under the dynamic event-triggered scheme, which reduces the total number of transmissions by 90.3% and reduces the number of transmissions by 8.9% compared to the static event-triggered scheme.

The system runs for 40 s and transmits data a total of 7200 times when the event-triggered scheme is not used. The two subsystems under the static event-triggered scheme transmit 4198 and 4199 times, respectively, which reduces the total number of transmissions by 41.7% while ensuring the system performance. In the dynamic event-triggered scheme as shown in Fig. 10a, the two subsystems transmit 1855 and 1834 times respectively, which reduces the total number of transmissions by 74.2%, and reduces the number of transmissions by 32.5% compared to the static event-triggered scheme, which indicates that with the growth of the system operation time, adopting the dynamic event-triggered scheme will be more advantageous than the static event-triggered scheme.

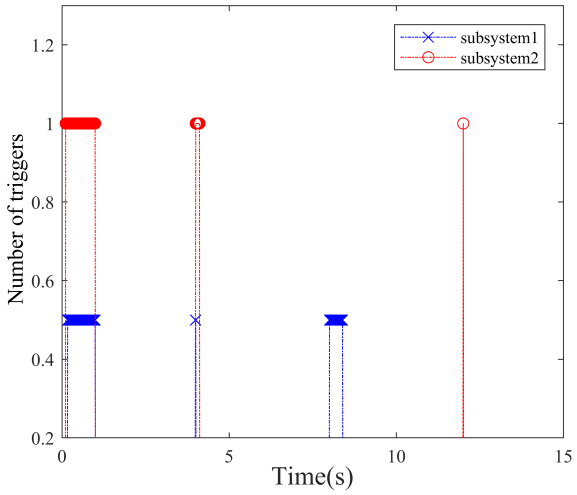

(a) Dynamic event-triggered mechanism

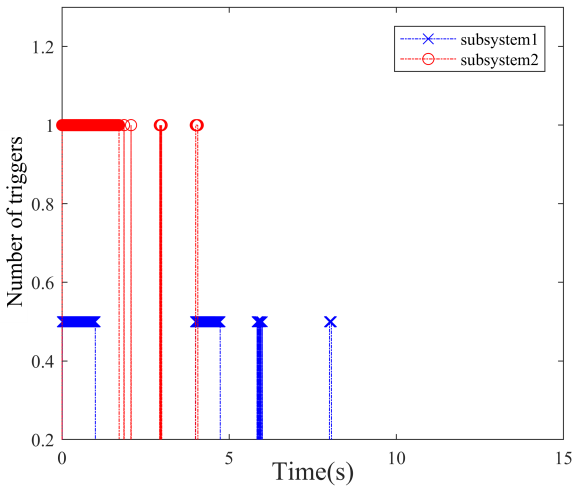

(b) Static event-triggered mechanism

Fig. 9. Number of triggers for dynamic event-triggered and static event-triggered in 15 s

Simulation results show that the robust fault-tolerant control method based on dynamic event-triggered designed in this paper can effectively reduce the number of data transmissions while ensuring the system performance. The trigger interval selected according to Theorem 3 can effectively avoid the Zeno behavior.

Remark 4. By introducing a positive real number r_0 into the dynamic event-triggered scheme, the triggering interval can be lengthened, and reduce the number of triggers. Meanwhile, the Zeno behavior can also be effectively prevented.

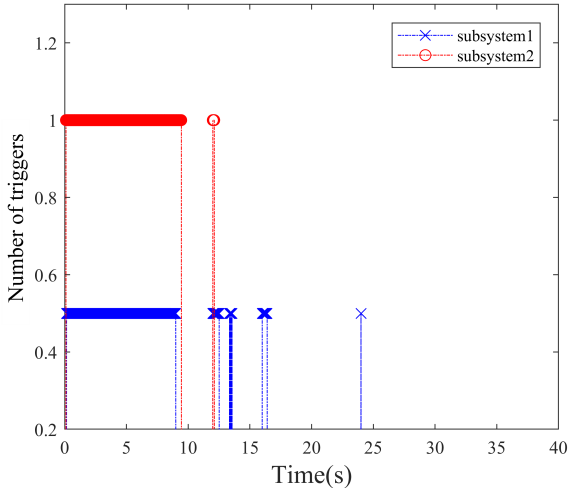

(a) Dynamic event-triggered mechanism

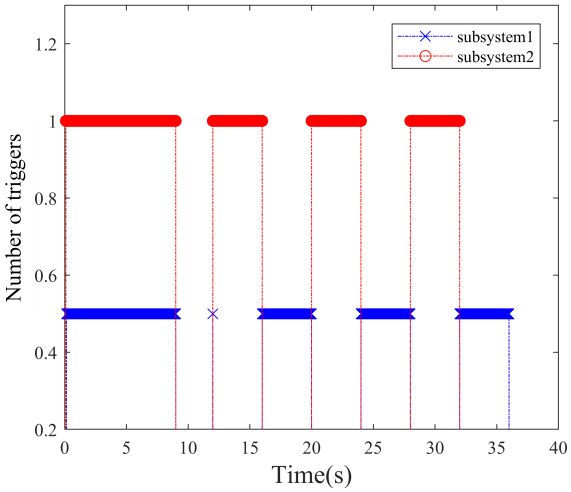

(b) Static event-triggered mechanism

Fig. 10. Number of triggers for dynamic event-triggered and static event-triggered in 40 s

6. CONCLUSIONS

In this paper, the design method of an adaptive observer and robust fault-tolerant controller is proposed for the nonlinear switched systems. An adaptive observer can simultaneously observe the system state and estimate system faults. Dynamic event-triggered condition is designed by exploiting the observed states. Under the robust fault-tolerant control, the switched system can be guaranteed to have good performance, while the number of samples and the transmission of unnecessary information can be greatly reduced. The gain matrices of the observer and controller can be obtained by solving the linear matrix inequality. Finally, the designed control strategy is applied to an aircraft model with switched wingspan curvature to verify its effectiveness.

ACKNOWLEDGEMENTS

This work is supported by the National Natural Science Foundation of China under Grant 61973041.

REFERENCES

[1] S. Song, J. Liu, and H. Wang, "Adaptive fault tolerant control for a class of nonlinear switched systems," *IEEE Access*, vol. 6, pp. 7728–7738, 2018.

[2] Y. Wang, N. Xu, Y. Liu, and X. Zhao, "Adaptive fault-tolerant control for switched nonlinear systems based on command filter technique," *Appl. Math. Comput.*, vol. 392, p. 125725, 2021.

[3] K. Zhang, B. Jiang, X. Yan, Z. Mao, and M.M. Polycarpou, "Fault-tolerant control for systems with unmatched actuator faults and disturbances," *IEEE Trans. Autom. Contr.*, vol. 66, no. 4, pp. 1725–1732, 2020.

[4] Y.-G. Zhou, S. Qi, and L.-N. Zhao, "Research and design of adaptive fault tolerant control based on actuator faults," in *2017 Chinese Automation Congress (CAC)*, IEEE, 2017, pp. 2793–2799.

[5] A.A. Ladel, A. Benzaouia, R. Outbib, and M. Ouladsine, "Robust fault tolerant control of continuous-time switched systems: An LMI approach," *Nonlinear Anal.-Hybrid Syst.*, vol. 39, p. 100950, 2021.

[6] J. Li, K. Pan, D. Zhang, and Q. Su, "Robust fault detection and estimation observer design for switched systems," *Nonlinear Anal.-Hybrid Syst.*, vol. 34, pp. 30–42, 2019.

[7] X. Liu, J. Han, H. Zhang, S. Sun, and X. Hu, "Adaptive fault estimation and fault-tolerant control for nonlinear system with unknown nonlinear dynamic," *IEEE Access*, vol. 7, pp. 136720–136728, 2019.

[8] M. Li, Y. Chen, L. Xu, and Z. Chen, "Asynchronous control strategy for semi-Markov switched system and its application," *Inf. Sci.*, vol. 532, pp. 125–138, 2020.

[9] Q. Lu, L. Zhang, P. Shi, and H.R. Karimi, "Control design for a hypersonic aircraft using a switched linear parameter-varying system approach," *Proc. Inst. Mech. Eng. Part I-J Syst Control Eng.*, vol. 227, no. 1, pp. 85–95, 2013.

[10] J. Jin, Y. Kim, S. Wee, D. Lee, and N. Gans, "A stable switched-system approach to collision-free wheeled mobile robot navigation," *J. Intell. Robot. Syst.*, vol. 86, pp. 599–616, 2017.

[11] J. Jin, J.-P. Ramirez, S. Wee, D. Lee, Y. Kim, and N. Gans, "A switched-system approach to formation control and heading consensus for multi-robot systems," *Intell. Serv. Robot.*, vol. 11, pp. 207–224, 2018.

[12] N. Noghredani and N. Pariz, "Robust adaptive control for a class of nonlinear switched systems using state-dependent switching," *SN Appl. Sci.*, vol. 3, pp. 1–10, 2021.

[13] X. Huo, H.R. Karimi, X. Zhao, B. Wang, and G. Zong, "Adaptive-critic design for decentralized event-triggered control of constrained nonlinear interconnected systems within an identifier-critic framework," *IEEE Trans. Cybern.*, vol. 52, no. 8, pp. 7478–7491, 2021.

[14] D. Yang, X. Li, J. Shen, and Z. Zhou, "State-dependent switching control of delayed switched systems with stable and unstable modes," *Math. Methods. Appl. Sci.*, vol. 41, no. 16, pp. 6968–6983, 2018.

[15] D. Yang, X. Li, and J. Qiu, "Output tracking control of delayed switched systems via state-dependent switching and dynamic output feedback," *Nonlinear Anal.-Hybrid Syst.*, vol. 32, pp. 294–305, 2019.

[16] X. Meng, D. Zhai, Z. Fu, and X. Xie, "Adaptive fault tolerant control for a class of switched nonlinear systems with unknown

control directions," *Appl. Math. Comput.*, vol. 370, p. 124913, 2020.

[17] R. Wang, L. Hou, G. Zong, S. Fei, and D. Yang, "Stability and stabilization of continuous-time switched systems: a multiple discontinuous convex Lyapunov function approach," *Int. J. Robust Nonlinear Control*, vol. 29, no. 5, pp. 1499–1514, 2019.

[18] X. Zhao, L. Zhang, P. Shi, and M. Liu, "Stability and stabilization of switched linear systems with mode-dependent average dwell time," *IEEE Trans. Autom. Control*, vol. 57, no. 7, pp. 1809–1815, 2011.

[19] Z. Yong, H. Fang, Y. Zheng, and X. Li, "Torus-event-based fault diagnosis for stochastic multirate time-varying systems with constrained fault," *IEEE Trans. Cybern.*, vol. 50, no. 6, pp. 2803–2813, 2019.

[20] H. Habbouche, Y. Amirat, T. Benkedjouh, and M. Benbouzid, "Bearing fault event-triggered diagnosis using a variational mode decomposition-based machine learning approach," *IEEE Trans. Energy Convers.*, vol. 37, no. 1, pp. 466–474, 2021.

[21] Y.-W. Wang, Y. Lei, T. Bian, and Z.-H. Guan, "Distributed control of nonlinear multiagent systems with unknown and nonidentical control directions via event-triggered communication," *IEEE Trans. Cybern.*, vol. 50, no. 5, pp. 1820–1832, 2019.

[22] J. Fu and T.-F. Li, *Event-Triggered Control of Switched Linear Systems*. Springer, 2021.

[23] Y. Wu, J. Zhang, and S. Fu, "Non-fragile event-triggered control of positive switched systems with random nonlinearities and controller perturbations," *Bull. Pol. Acad. Sci. Tech. Sci.*, vol. 69, pp. e138566, 2021.

[24] H. Ma, H. Li, R. Lu, and T. Huang, "Adaptive event-triggered control for a class of nonlinear systems with periodic disturbances," *Sci. China Inf. Sci.*, vol. 63, pp. 1–15, 2020.

[25] D. Ding, Z. Wang, and Q.-L. Han, "A set-membership approach to event-triggered filtering for general nonlinear systems over sensor networks," *IEEE Trans. Autom. Control*, vol. 65, no. 4, pp. 1792–1799, 2019.

[26] A. Girard, "Dynamic triggering mechanisms for event-triggered control," *IEEE Trans. Autom. Control*, vol. 60, no. 7, pp. 1992–1997, 2014.

[27] D. Ye, M.-M. Chen, and H.-J. Yang, "Distributed adaptive event-triggered fault-tolerant consensus of multiagent systems with general linear dynamics," *IEEE Trans Cybern*, vol. 49, no. 3, pp. 757–767, 2018.

[28] B. Liu, T. Liu, and P. Xiao, "Dynamic event-triggered intermittent control for stabilization of delayed dynamical systems," *Automatica*, vol. 149, p. 110847, 2023.

[29] Y. Gu, M. Shen, and C.K. Ahn, "Dynamic event-triggered fault-tolerant control through a new intermediate observer," *Int. J. Robust Nonlinear Control*, vol. 33, no. 16, pp. 9804–9825, 2023.

[30] D.-M. Li, X.-Q. He, L.-B. Wu, and Q.-K. Yu, "Event-triggered adaptive robust fault-tolerant control for a class of uncertain switched nonlinear systems," *Automatika*, vol. 64, no. 4, pp. 933–942, 2023.

[31] D. Cui and Z. Xiang, "Nonsingular fixed-time fault-tolerant fuzzy control for switched uncertain nonlinear systems," *IEEE Trans. Fuzzy Syst.*, vol. 31, no. 1, pp. 174–183, 2022.

[32] M.A. Ashraf, S. Ijaz, U. Javaid, S. Hussain, H. Anwaar, and M. Marey, "A robust sensor and actuator fault tolerant control scheme for nonlinear system," *IEEE Access*, vol. 10, pp. 626–637, 2021.

[33] Z. Zhu and J. Yu, "Anti-disturbance control of switching system and its application in Variant aircraft". M.Sc. thesis, Yangzhou University, China, 2022.